

2017

ETV2/ER71 regulates hematopoietic regeneration by promoting hematopoietic stem cell proliferation

Can-Xin Xu

Washington University School of Medicine in St. Louis

Tae-Jin Lee

Washington University School of Medicine in St. Louis

Nagisa Sakurai

Washington University School of Medicine in St. Louis

Karen Krchma

Washington University School of Medicine in St. Louis

Fang Liu

Washington University School of Medicine in St. Louis

See next page for additional authors

Follow this and additional works at: https://digitalcommons.wustl.edu/open_access_pubs

Recommended Citation

Xu, Can-Xin; Lee, Tae-Jin; Sakurai, Nagisa; Krchma, Karen; Liu, Fang; Li, Daofeng; Wang, Ting; and Choi, Kyunghee, "ETV2/ER71 regulates hematopoietic regeneration by promoting hematopoietic stem cell proliferation." *The Journal of Experimental Medicine*.214,6. 1643-1653. (2017).

https://digitalcommons.wustl.edu/open_access_pubs/5918

Authors

Can-Xin Xu, Tae-Jin Lee, Nagisa Sakurai, Karen Krchma, Fang Liu, Daofeng Li, Ting Wang, and Kyunghee Choi

ETV2/ER71 regulates hematopoietic regeneration by promoting hematopoietic stem cell proliferation

Can-Xin Xu,^{1,4} Tae-Jin Lee,¹ Nagisa Sakurai,¹ Karen Krchma,¹ Fang Liu,¹ Daofeng Li,² Ting Wang,² and Kyunghee Choi^{1,3}

¹Department of Pathology and Immunology, ²Department of Genetics, and ³Developmental, Regenerative, and Stem Cell Biology Program, Washington University School of Medicine, St. Louis, MO 63110

⁴The People's Hospital of Hunan Province and Hunan Normal University Institute for Clinical and Translational Science, Changsha, Hunan 410006, China

Recent studies have established that hematopoietic stem cells (HSCs) are quiescent in homeostatic conditions but undergo extensive cell cycle and expansion upon bone marrow (BM) transplantation or hematopoietic injury. The molecular basis for HSC activation and expansion is not completely understood. In this study, we found that key developmentally critical genes controlling hematopoietic stem and progenitor cell (HSPC) generation were up-regulated in HSPCs upon hematopoietic injury. In particular, we found that the ETS transcription factor Ets variant 2 (*Etv2*; also known as *Er71*) was up-regulated by reactive oxygen species in HSPCs and was necessary in a cell-autonomous manner for HSPC expansion and regeneration after BM transplantation and hematopoietic injury. We found *c-Kit* to be downstream of ETV2. As such, lentiviral *c-Kit* expression rescued *Etv2*-deficient HSPC proliferation defects in vitro and in short-term BM transplantation in vivo. These findings demonstrate that *Etv2* is an important regulator of hematopoietic regeneration.

INTRODUCTION

The hematopoietic system is remarkably sensitive to injury, including radiation or chemotherapy. As such, radiation can lead to lymphocyte, neutrophil, erythrocyte, and platelet loss, disruption of tissue homeostasis, and organismal death from infection and/or hemorrhage. Thus, rapid and effective regeneration of the hematopoietic system in response to injury is requisite for successful restoration of the hematopoietic tissue homeostasis and organismal survival. To this end, recent studies have demonstrated that hematopoietic stem cells (HSCs) rarely proliferate in steady states. However, they expand greatly after transplantation or injury to guarantee efficient restoration of the hematopoietic system (Sun et al., 2014; Busch et al., 2015; Säwén et al., 2016). As such, mechanistic understanding of such rapid hematopoietic stem and progenitor cell (HSPC) expansion would be beneficial for designing strategies achieving more efficient transplantation and hematopoietic regeneration.

ETS transcription factors have emerged as critical regulators of hematopoietic and vascular development (De Val and Black, 2009; Sumanas and Choi, 2016). In particular, *Etv2* (also known as *Er71* and *etsrp*) performs a nonredundant and indispensable function in hematopoietic and vessel development during embryogenesis, as *Etv2* deficiency leads to a complete block in hematopoietic and vascular formation and

embryonic lethality (Lee et al., 2008; Ferdous et al., 2009). Studies in zebrafish and *Xenopus laevis* have also demonstrated the critical function of *etv2* in blood and vessel formation (Sumanas and Lin, 2006; Sumanas et al., 2008; Neuhaus et al., 2010; Salanga et al., 2010). Importantly, *Etv2* is transiently expressed in the primitive streak, yolk sac blood islands, and large vessels including the dorsal aorta during embryogenesis (Lee et al., 2008; Kataoka et al., 2011; Rasmussen et al., 2011; Wareing et al., 2012). *Etv2* expression becomes undetectable once endothelial and hematopoietic cell lineages have been formed during embryogenesis. As such, hematopoietic and/or endothelial deletion of *Etv2* by using *Tie2-Cre*, *VEC-Cre*, or *Vav-Cre* leads to normal embryogenesis (Park et al., 2016), supporting the notion that *Etv2* is only transiently required for the vessel and blood cell lineage formation. Consistently, *Etv2* deletion by using *Flk1-Cre* leads to embryonic lethality because of insufficient hemangiogenic progenitor generation (Liu et al., 2015). Mechanistically, ETV2 positively activates genes critical for hematopoietic and endothelial cell lineage specification (Liu et al., 2012, 2015).

Despite its essential function in hematopoietic and vascular cell lineage development, studies investigating its role in adult hematopoiesis have been limiting. Notably, *Etv2* deletion using the *Mx1-Cre* system and polyinosinic:polycytidylic acid (pIpC) administration led to seemingly rapid loss of HSC number and their hematopoietic reconstitution potential (Lee et al., 2011). Although this

Correspondence to Kyunghee Choi: kchoi@wustl.edu

N. Sakurai's present address is Astellas Pharma Inc., Chuo-ku, Tokyo 103-8411, Japan.

Abbreviations used: 5-FU, 5-fluorouracil; CHIP-Seq, chromatin immunoprecipitation sequencing; HSC, hematopoietic stem cell; HSPC, hematopoietic stem and progenitor cell; NAC, *N*-acetyl cysteine; PB, peripheral blood; ROS, reactive oxygen species; SLAM, signaling lymphocytic activation molecule.



study suggested its role in maintaining hematopoiesis in steady states, *Tie2-Cre* (hematopoietic and endothelial)– or *Vav-Cre* (hematopoietic)–mediated *Etv2* deletion resulted in no appreciable hematopoietic phenotypes in steady states (Park et al., 2016). As the severe phenotype observed by Lee et al. (2011) could be caused by the combined effect between *Etv2* loss and pIpC treatment, which perturbs steady-state hematopoiesis (Essers et al., 2009; Sato et al., 2009), we determined whether *Etv2* might have an unexpected role in non-steady-state hematopoiesis. Specifically, we characterized hematopoietic regeneration in *Etv2*-deficient mice by using BM transplantation and 5-fluorouracil (5-FU)–mediated hematopoietic injury models. Our study demonstrated that although *Etv2* was not essential for homeostatic hematopoiesis, it was reactivated upon injury and was required for HSPC proliferation to rapidly restore the hematopoietic system. We identify reactive oxygen species (ROS) as an upstream factor that activates *Etv2* in injury. Without *Etv2*, HSPCs failed to expand, and mice succumbed to hematopoietic failure and death, revealing a critical role of this factor in hematopoietic regeneration. Importantly, we identify *c-Kit* as a downstream target that could rescue proliferation defects of the *Etv2*-deficient HSPCs in vitro and in short-term BM transplantation in vivo.

RESULTS AND DISCUSSION

Etv2 is activated upon hematopoietic injury through ROS

We previously reported that mature blood (B220⁺, Mac1⁺, Gr1⁺, Ter119⁺, CD4⁺, and CD8⁺) and HSPC (*c-KIT*⁺Sca1⁺Lin⁻ [KSL]) cell populations in *Tie2-Cre;Etv2^{fl/fl}* (herein *Tie2-Cre;Etv2* CKO) mice were present at similar levels compared with controls (Park et al., 2016). Additional analysis for the frequency and absolute number of the lineage negative (Lin⁻), *c-KIT*⁺Sca1⁻Lin⁻ (LK; progenitor cell) and the CD150⁺CD48⁻KSL (KSL-SLAM [signaling lymphocytic activation molecule]; HSC) cell population in *Tie2-Cre;Etv2* CKO BM revealed that they were also comparable with those of the littermate control mice (not depicted). Similarly, the common myeloid progenitor (CD34⁺CD16/32⁻LK), granulocyte-macrophage progenitor (CD34⁺CD16/32⁺LK), and megakaryocyte-erythrocyte progenitor (CD34⁻CD16/32⁺LK) cell populations were also comparable in *Tie2-Cre;Etv2* CKO and control BM (not depicted). These findings support the notion that *Etv2* was dispensable for maintaining homeostatic hematopoiesis.

To determine whether *Etv2* plays a role in nonhomeostatic conditions, we assessed whether its expression was activated in HSPCs after hematopoietic injury, assuming its activation would have a role in regeneration. In particular, we assessed BM response to 5-FU treatment, as it depletes cycling hematopoietic cells and activates quiescent HSCs to proliferate and self-renew. Upon 5-FU injury, cycling hematopoietic cells are rapidly lost (days 1–5), hematopoietic regeneration ensues (days 6–11), and then homeostasis is re-established (after day 20). Unexpectedly, *Etv2* expression was

readily detected in HSPCs, not in more committed progenitor cells (Lin⁻*c-Kit*⁺Sca1⁻; not depicted), when examined 10 d after 5-FU injection (Fig. 1 A). Additional key transcription factors controlling HSPC generation in development, *Gata2*, *Scl*, *Fli1*, and *Runx1*, were also up-regulated (Fig. 1 A). Importantly, the kinetics of expression of these key genes, *Etv2*, *Gata2*, and *Scl*, coincided with that of the regeneration phase (Fig. 1 B). As tissue injury leads to ROS production and ROS is required for tissue regeneration (Gauron et al., 2013; Love et al., 2013), we determined whether 5-FU injury leads to ROS production and *Etv2* activation in HSPCs. Remarkably, ROS levels were elevated in HSPCs during the regeneration phase after 5-FU treatment (days 9 and 10) but returned to normal levels by day 11 and remained low for the duration of the study (after day 13; Fig. 1 C). We saw slightly higher levels of ROS in *Etv2*-deficient HSPCs compared with controls at day 9, presumably because of proliferation defects in *Etv2*-deficient HSPCs leading to accumulation of the ROS generated (see the next section). Importantly, L-buthionine-S,R-sulfoximine (BSO), an inhibitor of glutathione biosynthesis, which leads to ROS production, increased intracellular ROS levels and *Etv2* expression in HSPCs, suggesting that 5-FU injury leads to ROS production and *Etv2* up-regulation in HSPCs (Fig. 1, D and E). Indeed, *Etv2* expression remained low in HSPCs when N-acetyl cysteine (NAC; ROS scavenger) and apocynin (NADPH [nicotinamide adenine dinucleotide phosphate reduced] oxidase inhibitor) were administered during recovery phase after 5-FU injury, demonstrating that ROS is upstream of *Etv2* activation upon injury (Fig. 1 F).

Hematopoietic *Etv2* but not endothelial *Etv2* is critical for HSPC regeneration after 5-FU injury

To evaluate the significance of the *Etv2* activation in the regeneration capacity of HSPCs, we assessed the HSPC recovery potential in *Tie2-Cre;Etv2* CKO mice after 5-FU injury (250 mg/kg). No significant difference in the BM cellularity was observed after 5-FU injection between control and CKO mice (not depicted). Whereas the KSL and CD150⁺CD48⁻KSL absolute cell number and frequency in control mice recovered by 11 d after 5-FU injury and reached homeostatic levels by day 21, *Tie2-Cre;Etv2* CKO BM had reduced levels of HSPCs at days 10 and 11 (Fig. 2, A and B; Fig. S1). Despite the reduced HSPC recovery rate, HSPCs in *Tie2-Cre;Etv2* CKO mice also reached the homeostatic levels by day 21 (Fig. 2, A and B). The reduced HSPC frequency during the recovery phase, days 10 and 11, suggested lower proliferation rate of HSPCs. Thus, we assessed whether *Etv2* deletion impacted HSPC proliferation. Specifically, we performed Ki67 and DAPI staining to determine the cell cycle status of the *Etv2*-deficient HSPCs. The percentage of KSL cells in the S-G2-M phase was slightly less, but statistically significant, in *Tie2-Cre;Etv2* CKO mice compared with control mice at day 9 after 5-FU injury (Fig. 2 C). By day 10, *Etv2*-deficient KSL cells had a similar percentage of cells in the S-G2-M phase compared with controls. Notably, the

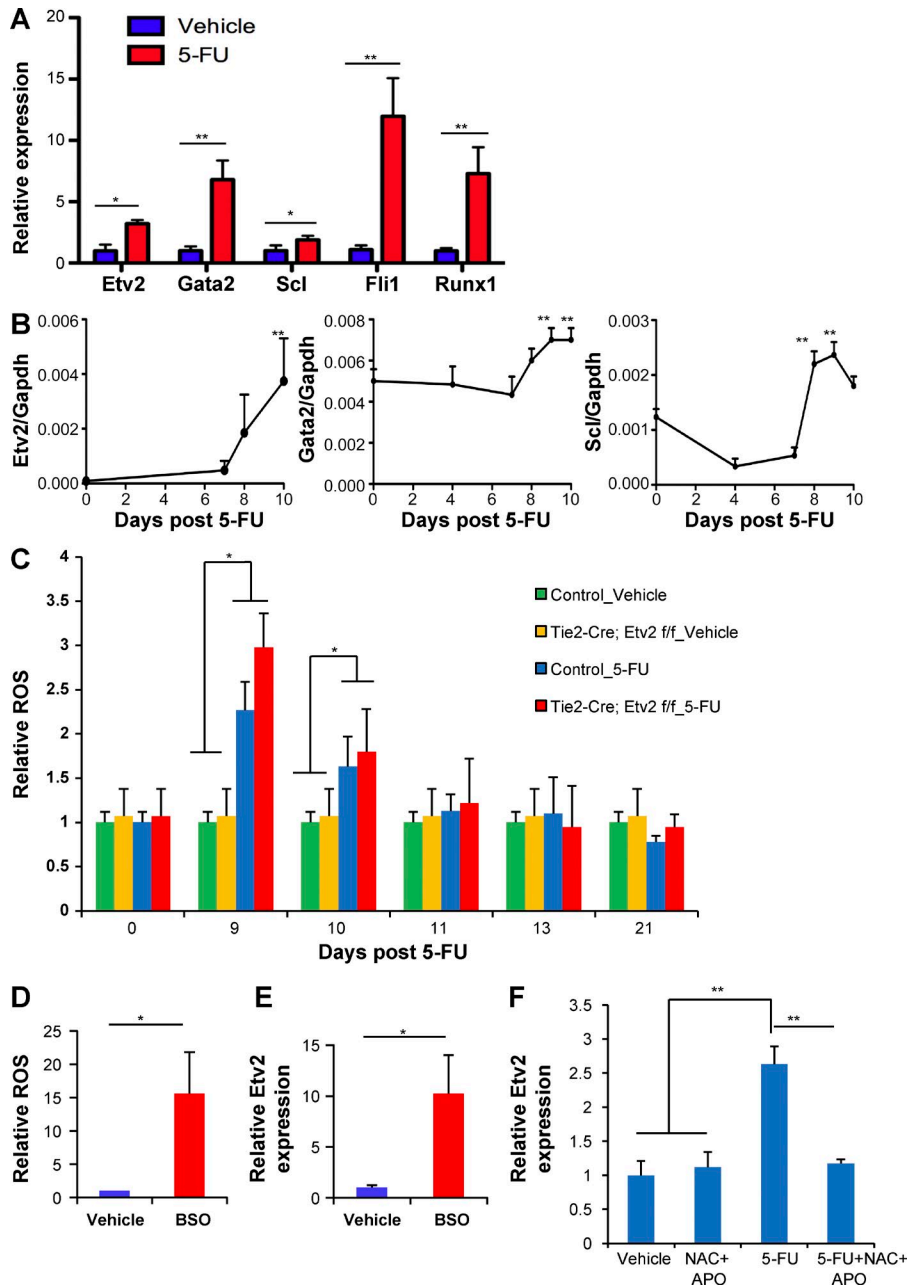


Figure 1. Etv2 is activated upon hematopoietic injury through ROS.

(A) KSL cells were sorted from WT mice 10 d after vehicle (PBS) or 250 mg/kg 5-FU injection i.p. 20,000–40,000 pooled KSL cells from each sample were subjected to RNA extraction and real-time PCR. Data are shown as a relative expression of *Etv2*, *Gata2*, *Scl*, *Fli1*, and *Runx1* normalized to the vehicle-treated control group. $n = 9$ from three independent experiments. (B) KSL cells were sorted at the indicated time points after 250 mg/kg 5-FU injection i.p. 20,000–40,000 pooled KSL cells (*Etv2*) or whole BM (*Scl* and *Gata2*) were subjected to RNA extraction and real-time PCR. *Etv2*, *Gata2*, and *Scl* expression normalized to GAPDH is shown. $n = 4–6$ from two independent experiments. (C) Tie2-Cre;*Etv2* CKO mice or littermate control mice were injected with 250 mg/kg 5-FU i.p. or vehicle (PBS). DCFDA staining was performed on KSL cells from days 0, 9, 10, 11, 13, and 21 after 5-FU injection. Data are expressed as a relative ROS level normalized to the littermate control day-0 group. $n = 6–9$ from two independent experiments. (D and E) 40,000 KSL cells were cultured in a 24-well plate for 2 d with 10 μ M BSO or vehicle, followed by DCFDA staining or real-time PCR analysis. Relative ROS levels and *Etv2* expression in KSL cells were normalized to the vehicle control group. $n = 6$ from two independent experiments. (F) WT mice were injected with 250 mg/kg 5-FU i.p. or vehicle. Mice were treated with NAC and apocynin (APO) from days 4–10. 1 mg/ml NAC was added in the drinking water (changed every 3 d). 50 mg/kg apocynin was injected i.p. every day for 6 d starting from day 4. At day 10, 20,000–40,000 KSL cells were sorted for RNA extraction and quantitative RT-PCR. Data are expressed as a relative *Etv2* expression normalized to the vehicle control group. $n = 6$ from two independent experiments. *, $P < 0.05$; **, $P < 0.01$. Error bars indicate standard error of the mean.

percentage of CD150⁺CD48⁻KSL cells in the S-G2-M phase was greatly reduced in Tie2-Cre;*Etv2* CKO mice during the recovery period after 5-FU injury (Fig. 2 D). These cells were mainly in the quiescent state (Fig. 2 E), suggesting that *Etv2* is required for promoting HSC proliferation and regeneration.

The appreciable proliferation potential of the *Etv2*-deficient HSPC population (KSL; Fig. 2, A and C) suggested that peripheral blood (PB) might recover relatively normally in Tie2-Cre;*Etv2* CKO after 5-FU injury. Indeed, complete blood cell count data showed no substantial differences of the PB cell recovery between Tie2-Cre;*Etv2* CKO and control mice after 5-FU injection (Fig. 2, F and G). BM

and PB lineage analysis also showed that the frequency of B cells (B220⁺), T cells (CD3⁺), and myeloid cells (Gr1⁺ and Mac1⁺) was comparable between Tie2-Cre;*Etv2* CKO and littermate controls (not depicted). However, we noticed that white blood cell counts in Tie2-Cre;*Etv2* CKOs were lower at day 14 after 5-FU injury (Fig. 2 F). Moreover, about one half of the 5-FU-injected Tie2-Cre;*Etv2* CKO mice, but not control mice, died after repeated blood drawing for PB analysis (not depicted). As the most primitive hematopoietic cell population displayed a notable defect in cell cycle/proliferation, it was possible that Tie2-Cre;*Etv2* CKO mice might not manage stress requiring continued hematopoietic regeneration.

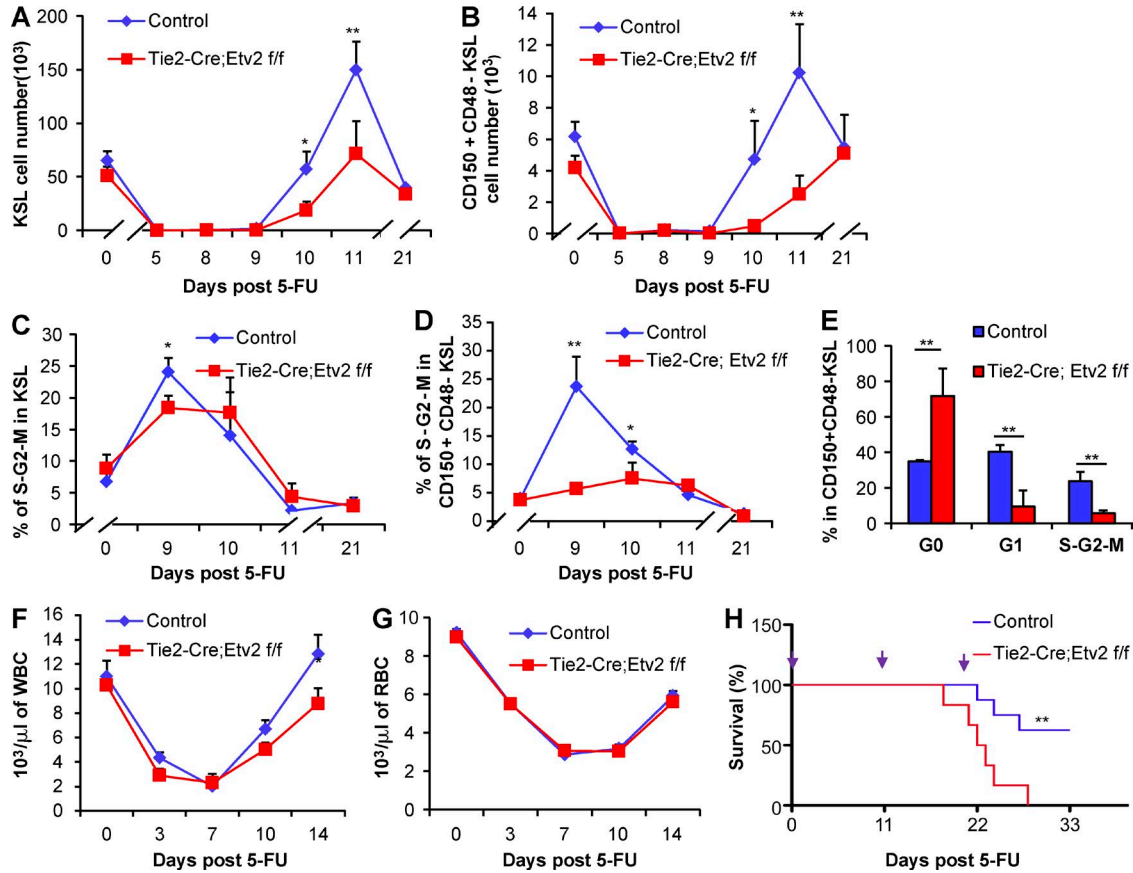


Figure 2. Impaired hematopoietic regeneration in *Tie2-Cre;Etv2* CKO mice after 5-FU treatment. (A–H) *Tie2-Cre;Etv2* CKO mice or littermate control mice were injected with 250 mg/kg 5-FU i.p. or vehicle. (A and B) At days 0, 5, 8, 9, 10, 11, and 21 after 5-FU injection, the absolute number (per femur and tibia) of KSL or KSL-SLAM cells was determined by flow cytometry. $n = 6$ from two independent experiments. (C and D) At days 0, 9, 10, 11, and 21 after 5-FU injection, the percentage of G0, G1, and S-G2-M phases in KSL or KSL-SLAM (CD150⁺CD48⁻ KSL) was determined by flow cytometry using surface markers Ki67 and DAPI staining. $n = 6$ from two independent experiments. (E) Cell cycle analysis of KSL-SLAM cells is shown at day 9. $n = 6$ from two independent experiments. (F and G) Complete blood cell count was analyzed by a Hemavet 950FS hematology system at days 0, 3, 7, 10, and 14 after 5-FU injection to determine white blood cells (WBCs) and RBCs. $n = 10$ from two independent experiments. (H) *Tie2-Cre;Etv2* CKO mice and littermate control mice were injected with 250 mg/kg 5-FU i.p. for three times at an 11-d interval, and survival was monitored daily. A Kaplan-Meier survival curve of mice after 5-FU injury is shown. Time points of 5-FU injections are indicated on top with purple arrows. $n = 10$ from two independent experiments. *, $P < 0.05$; **, $P < 0.01$. Error bars indicate standard error of the mean.

Thus, we tested whether *Etv2*-deficient HSC proliferation defects could be manifested by repeated 5-FU injury. Specifically, we applied serial injection of 250 mg/kg 5-FU at an 11-d interval, an interval that showed maximal HSPC expansion in WT mice (Fig. 2, A–D), to continuously induce HSCs into cell cycle/proliferation. *Tie2-Cre;Etv2* CKO mice started to die after the second 5-FU injection, and all mice died after the third 5-FU injection. In contrast, less than half of the control mice died after the third 5-FU injection (Fig. 2 H). At a less cytotoxic dose of 5-FU (150 mg/kg), 1 out of 10 *Tie2-Cre;Etv2* CKO mice died after the third 5-FU injection, whereas none of the littermate control mice died (not depicted). At a lower 5-FU dose (150 mg/kg), ROS levels were not significantly elevated in HSPCs, and *Etv2*-deficient HSPCs proliferated comparably with those from littermate

controls (not depicted). These data suggested that, at extreme hematopoietic stress conditions, *Etv2*-deficient HSPCs, being defective in proliferative potential, might not meet the demands of rapid restoration of the hematopoietic system.

To determine that the effect of *Etv2* on HSPC proliferation was hematopoietic cell intrinsic, we assessed the hematopoietic regeneration potential of *Vav-Cre;Etv2*^{f/f} (*Vav-Cre;Etv2* CKO) and *VECadherin-Cre;Etv2*^{f/f} (*VEC-Cre;Etv2* CKO) mice, which lack *Etv2* in hematopoietic and endothelial cells, respectively (Park et al., 2016). *Etv2* deletion was confirmed in BM CD45⁺ as well as KSL cells in both *Vav-Cre;Etv2* and *Tie2-Cre;Etv2* CKO mice but not in *VEC-Cre;Etv2* CKO mice (not depicted). Additionally, complete *Etv2* deletion was observed in CD31⁺CD45⁻ endothelial cells isolated from *Tie2-Cre;Etv2* or *VEC-Cre;Etv2*

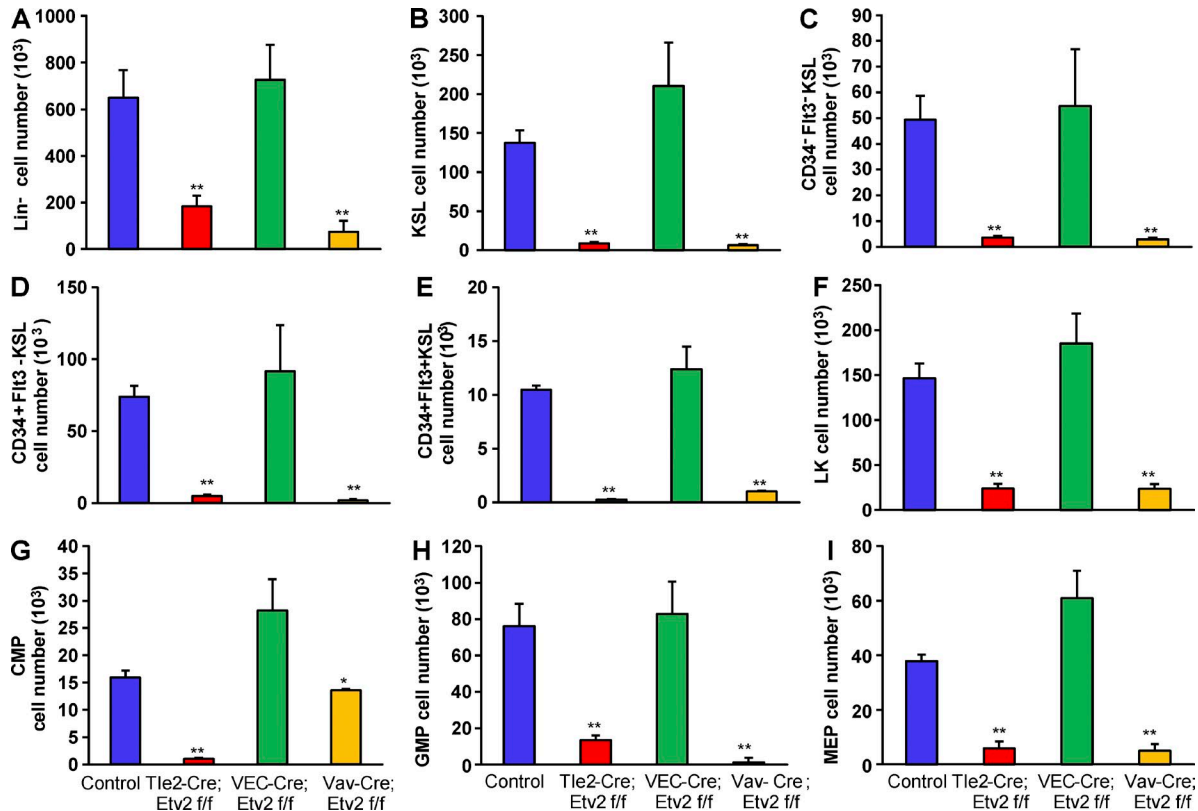


Figure 3. Hematopoietic but not endothelial deletion of *Etv2* impairs HSPC recovery after 5-FU treatment. (A–I) Tie2-Cre;*Etv2* CKO, VEC-Cre;*Etv2* CKO, *Vav-Cre*;*Etv2* CKO, or littermate control mice were injected with 250 mg/kg 5-FU i.p. After 11 d, BM mononuclear cells were subjected to flow cytometry by using HSPC surface markers to determine absolute cell number (per femur and tibia) of different hematopoietic compartments. (A) Lin⁻ cells. (B) KSL (c-Kit⁺Sca1⁺Lin⁻) cells. (C) Long-term HSCs (CD34⁻Flt3⁻ KSL). (D) Short-term HSCs (CD34⁺Flt3⁻ KSL). (E) Multipotent progenitor (CD34⁺Flt3⁺ KSL) cells. (F) LK (c-Kit⁺Sca1⁻Lin⁻) cells. (G) Common myeloid progenitor (CMP; CD34⁺CD16/32⁻ LK) cells. (H) Granulocyte-macrophage progenitor (GMP; CD34⁺CD16/32⁺ LK) cells. (I) Megakaryocyte-erythrocyte progenitor (MEP; CD34⁻CD16/32⁻ LK) cells. $n = 4-6$ from two independent experiments. *, $P < 0.05$; **, $P < 0.001$. Error bars indicate standard error of the mean.

CKO lungs (not depicted). *Etv2* deletion in KSL cells was not complete in *Tie2-Cre*;*Etv2* CKO mice, even though these mice showed significantly diminished hematopoietic regeneration capacity. After 5-FU injury, BM cellularity was similar between control and CKO mice (not depicted). Importantly, *Vav-Cre*;*Etv2* CKO mice displayed similar HSPC recovery defects compared with *Tie2-Cre*;*Etv2* CKO mice. *VEC-Cre*;*Etv2* CKO mice exhibited comparable HSPC recovery as control mice (Fig. 3). These data suggest that hematopoietic *Etv2* but not endothelial *Etv2* is required for HSPC regeneration after 5-FU injury.

Hematopoietic *Etv2* but not endothelial *Etv2* is essential for hematopoietic reconstitution after transplantation

To further validate the hematopoietic cell-intrinsic role of *Etv2* in HSPC regeneration, we used BM transplantation, which stimulates continuous long-term proliferation of HSPCs (Sun et al., 2014; Busch et al., 2015; Säwén et al., 2016), to assess *Etv2*-deficient HSPCs for their hematopoietic reconstitution potential. Specifically, we performed competi-

tive transplantation experiments by mixing KSL cells from *Vav-Cre*;*Etv2* CKO mice (CD45.2) and WT mice (CD45.1) at a 1:1 ratio and injecting them into lethally irradiated recipients (CD45.1 × 45.2). *Vav-Cre*;*Etv2* CKO KSL cells (CD45.2) showed very low PB contribution compared with competitive controls (Fig. 4, A and B). *Vav-Cre*;*Etv2* CKO BM cells from the primary recipients showed similar defects in hematopoietic reconstitution in secondary transplantation (not depicted). Whole BM transplantation using *Vav-Cre*;*Etv2* CKO (CD45.2) and WT (CD45.1) mice (1:1 ratio) again showed very low PB contribution from *Vav-Cre*;*Etv2* CKO mice compared with controls (not depicted). *Etv2*-deficient HSPCs displayed similar homing ability compared with WT HSPCs when injected retroorbitally and analyzed 4 h and 2 d after transplantation (not depicted). These data indicated that hematopoietic *Etv2* was required for hematopoietic reconstitution after transplantation.

To enforce the notion that *Etv2* was required for the HSC-intrinsic manner, we performed competitive hematopoietic reconstitution studies by using *VEC-Cre*;*Etv2* CKO

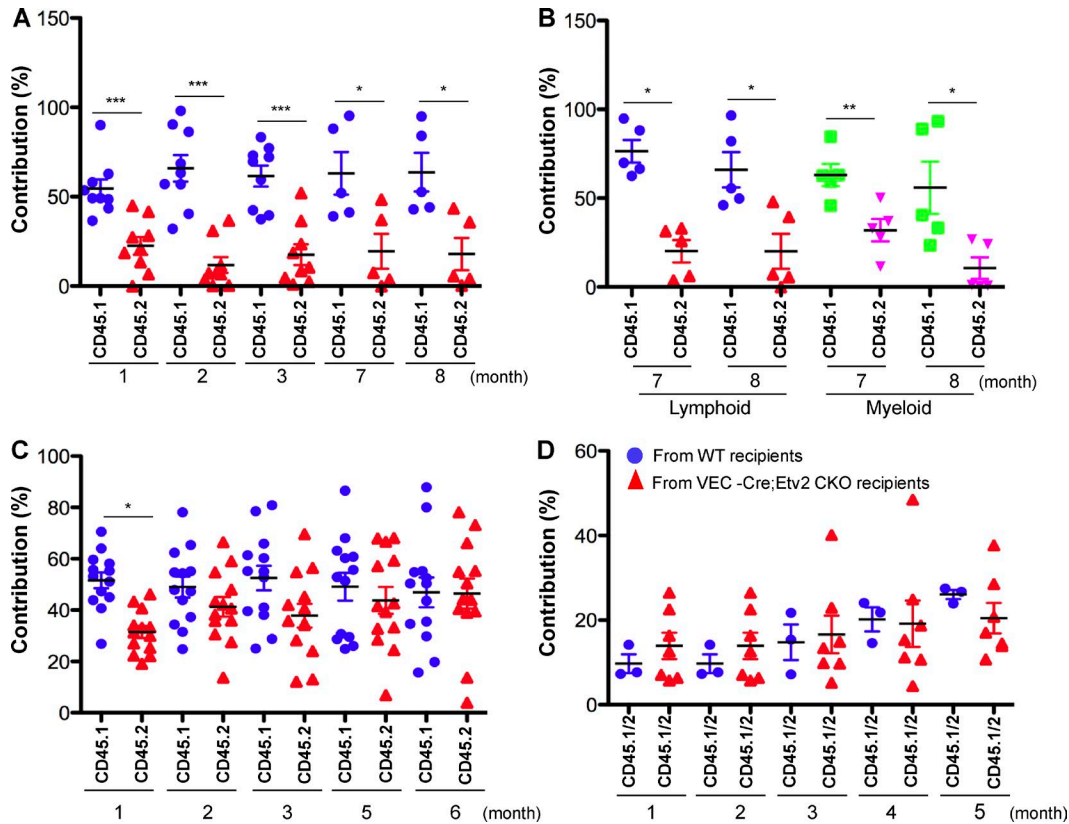


Figure 4. Hematopoietic but not endothelial deletion of *Etv2* results in decreased hematopoietic reconstitution capacity. (A and B) 10,000 KSL cells from *Vav-Cre;Etv2* CKO or littermate control mice (both are CD45.2) were transplanted along with 10^6 competitor BM cells (CD45.1) into lethally irradiated WT recipient mice (CD45.1 \times CD45.2). PB from recipients was analyzed for donor-derived contribution by determining the percentage of CD45.1⁺ and CD45.2⁺ PB leukocyte or lymphoid (B220⁺/CD3⁺ or myeloid Gr1⁺) at the indicated time points after transplantation. $n = 5-8$ from two independent transplantations. (C) 10^6 BM cells from *VEC-Cre;Etv2* CKO or littermate control mice (both are CD45.2) were transplanted along with 10^6 competitor BM cells (CD45.1) into lethally irradiated WT recipient mice (CD45.1 \times CD45.2). PB from recipients was analyzed for donor-derived contribution by determining the percentage of CD45.1⁺ and CD45.2⁺ PB leukocytes at the indicated time points after transplantation. $n = 10-13$ from three independent transplantations. (D) 2×10^6 WT BM cells (CD45.1 \times CD45.2) were transplanted into lethally irradiated WT or *VEC-Cre;Etv2* CKO recipients (both are CD45.2). 6 mo after transplantation, 2×10^6 BM cells (CD45.1 \times CD45.2) recovered from WT or *VEC-Cre;Etv2* CKO recipients were transplanted along with 5×10^5 competitor BM cells (CD45.1) into lethally irradiated recipient mice (CD45.2). PB was analyzed for donor-derived contribution by determining the percentage of CD45.1⁺CD45.2⁺ PB leukocytes at the indicated time points after transplantation. $n = 3-6$ from two independent experiments. *, $P < 0.05$; **, $P < 0.01$; ***, $P < 0.001$.

BM (CD45.2) and WT BM (CD45.1) cells (1:1 ratio) and lethally irradiated recipient mice (CD45.1 \times 45.2). PB analysis showed that *VEC-Cre;Etv2* CKO BM cells (CD45.2) had comparable contribution to PB compared with controls (Fig. 4 C). To further validate that endothelial *Etv2* was dispensable for HSPC regeneration potential, we additionally performed transplantation studies using WT BM (CD45.1 \times 45.2) as the donor and lethally irradiated WT (CD45.2) or *VEC-Cre;Etv2* CKO mice (CD45.2) as recipients. 6 mo later, WT donor BM (CD45.1 \times 45.2) was recovered from the WT or *VEC-Cre;Etv2* CKO-recipient mice, mixed with fresh WT BM (CD45.1) in a ratio of 4:1, and transplanted into lethally irradiated recipients (CD45.2). PB analysis showed that WT BM (CD45.1 \times 45.2) recovered from the *VEC;Etv2* CKO mice had similar contribution compared with the WT BM (CD45.1 \times 45.2) recovered from the WT

mice (Fig. 4 D). These data demonstrate that endothelial *Etv2* was not required for maintaining HSPC function.

c-KIT signaling is downstream of ETV2 in promoting HSPC proliferation and recovery from 5-FU injury

To understand the molecular mechanisms by which *Etv2* regulates HSC regeneration, we examined previously published chromatin immunoprecipitation sequencing (ChIP-Seq) and microarray data (Liu et al., 2012, 2015) focusing on the genes in the regulation of cell proliferation categories. A great fraction of the ETV2 ChIP-Seq peaks were associated with genes annotated as regulation of cell proliferation by gene ontology (McLean et al., 2010), whose expression also changed by ETV2 status (Fig. 5 A). Among these, *c-Kit* expression was greatly up-regulated by enforced *Etv2* expression, whereas its expression was significantly decreased by *Etv2* deficiency

(Fig. 5 B). ChIP-Seq data also identified potential ETV2 binding sites in the *c-Kit* locus (Fig. S2), suggesting that *c-Kit* is downstream of ETV2. Thus, we determined whether ETV2-mediated *c-Kit* up-regulation was required for hematopoietic regeneration after BM injury. FACS analyses of the recovering BM after 5-FU injury demonstrated that c-KIT expression was dramatically up-regulated in Lin⁻ cells during the regeneration phase in control mice (Fig. 5 C). Notably, its expression returned to normal levels once the hematopoietic system was restored, i.e. day 21. However, c-KIT expression levels in Lin⁻ cells remained low during the recovery phase in *Tie2-Cre;Etv2* CKO BM (Fig. 5 C). Baseline c-KIT expression in steady state was similar (not depicted). In culture, c-KIT⁺ cells had much higher proliferation rate than c-KIT⁻ cells (Fig. 5 D). This suggested that *Etv2* deficiency leads to defects in *c-Kit* up-regulation and c-KIT-mediated HSPC proliferation. To determine whether *Etv2*-mediated c-KIT up-regulation was indeed required for HSPC proliferation and hematopoietic regeneration after BM injury, we tested whether *c-Kit* expression could rescue the HSPC proliferation defects of the *Tie2-Cre;Etv2* CKO BM. To this end, *Tie2-Cre;Etv2* BM cells were isolated 8 d after 5-FU injury and infected with *Etv2* or *c-Kit* lentivirus, and c-KIT expression, proliferation, and cell cycle of the infected cells were analyzed. As expected, *Etv2* lentiviral infection dramatically rescued the frequency and numbers of c-KIT⁺ cells (Fig. 5, E–G). Moreover, *c-Kit* lentiviral infection also led to increased c-KIT⁺ cell frequency and numbers from the *Etv2*-deficient BM. To determine whether the rescue of the cell-surface phenotype, c-KIT⁺ cells, indeed reflected the functional rescue of the proliferation defects, we assessed BM cell recovery as well as the cell-cycle status of the *c-Kit*-infected cells. BM cell recovery and proliferation were significantly improved by *Etv2* or *c-Kit* expression in *Etv2*-deficient BM (Fig. 5, E–G). Moreover, *Etv2*-deficient BM cells yielded a much higher percentage of cells in the S-G2-M phase after *Etv2* or *c-Kit* lentiviral infection (Fig. 5 G). As expected, highly proliferating cells, i.e. cells in the S-G2-M phase, were enriched within c-KIT⁺ cells generated by *Etv2* or *c-Kit* expression (Fig. 5 D). To determine whether *c-Kit* could rescue *Etv2*-deficient HSC defects in vivo, we collected *Etv2*-deficient BM cells 7 d after 5-FU injury (CD45.2), infected them with *Venus*, *Etv2*, or *c-Kit* lentivirus, transplanted them into lethally irradiated recipient mice (CD45.1) together with mock-infected WT BM (CD45.1), and then analyzed them 3 d later for the total BM contribution and c-KIT⁺ cells generated. As shown (Fig. 5, H and I; and Fig. S3), total donor contribution (CD45.2⁺) as well as CD45.2⁺c-KIT⁺ cells were increased by either *Etv2* or *c-Kit* expression compared with *Venus* control. These data collectively support the notion that c-KIT-mediated HSPC proliferation was integral to ETV2-mediated BM recovery after injury.

In the present study, we uncover the unexpected role of *Etv2* in hematopoietic regeneration. Upon hematopoietic injury, we discover that ROS levels are transiently increased

in HSPCs and that *Etv2* becomes transiently reactivated in HSPCs. Inhibition of ROS was sufficient to block *Etv2* activation in HSPCs upon injury. *Etv2* was necessary to ensure efficient hematopoietic regeneration after hematopoietic injury. As such, we propose that although *Etv2* is dispensable for maintaining HSCs in steady states, it is required for emergency hematopoiesis. Surprisingly, despite its critical role in vascular regeneration (Park et al., 2016), we found that *Etv2* was dispensable in the endothelial cell niche for maintaining HSCs in the steady state or injury.

Recent studies have established that ROS is critical for tissue regeneration. In particular, in the *Xenopus* tadpole tail regeneration model, tail amputation leads to rapid ROS production, which activates Wnt/ β -catenin and FGF20 signaling and tail regeneration (Love et al., 2013). In the zebrafish fin-amputation regeneration model, ROS is again rapidly produced in regenerating tissue and triggers compensatory proliferation of stump epidermal cells (Gauron et al., 2013). ROS positively regulate mouse spermatogonial stem cell self-renewal through stress kinases p38 MAPK and JNK pathways (Morimoto et al., 2013). ROS is also required for neuroregeneration in newts and planarian (Hameed et al., 2015; Piroette et al., 2015). Intriguingly, ROS role in HSCs seem controversial (Ito et al., 2006; Ludin et al., 2014; Walter et al., 2015; Itkin et al., 2016). In particular, activation of the ROS–p38 MAPK pathway appears to be detrimental for HSCs (Ito et al., 2006; Walter et al., 2015). However, a conditional p38 α deletion study has revealed that it is necessary for HSC regeneration in stress response (Karigane et al., 2016). It is important to note that ROS levels were transiently elevated in HSPCs during regeneration phase, which might be the key to successful HSC regeneration. Future studies will require detailed mechanistic understanding of ROS and *Etv2* activation in relationship to p38 MAPK that contributes to hematopoietic regeneration.

KIT ligand and c-KIT interaction between the stromal niche and HSCs is critical for maintaining HSPCs in adults (Geissler et al., 1988; Huang et al., 1990; Matsui et al., 1990; Thorén et al., 2008; Kimura et al., 2011; Ding et al., 2012). Importantly, c-KIT levels on HSCs determine the outcome of the HSC fate (Grinenko et al., 2014; Shin et al., 2014). Specifically, HSCs expressing high levels of c-KIT cannot contribute to long-term hematopoietic reconstitution, as they proliferate more robustly and differentiate upon transplantation. However, HSCs with low levels of c-KIT were able to contribute to long-term hematopoietic reconstitution. Our data suggest that *c-Kit* is downstream of ETV2 and responsible for HSPC proliferation during hematopoietic recovery. In particular, c-KIT expression remained low in *Etv2*-deficient HSPCs during recovery, and the *c-Kit* gene delivery could rescue proliferation defects of *Etv2*-deficient HSPCs in vitro and in short-term BM transplantation in vivo. However, *c-Kit* gene delivery failed to rescue the long-term repopulation potential of *Etv2*-deficient HSPCs (unpublished data). This outcome is reminiscent of the stud-

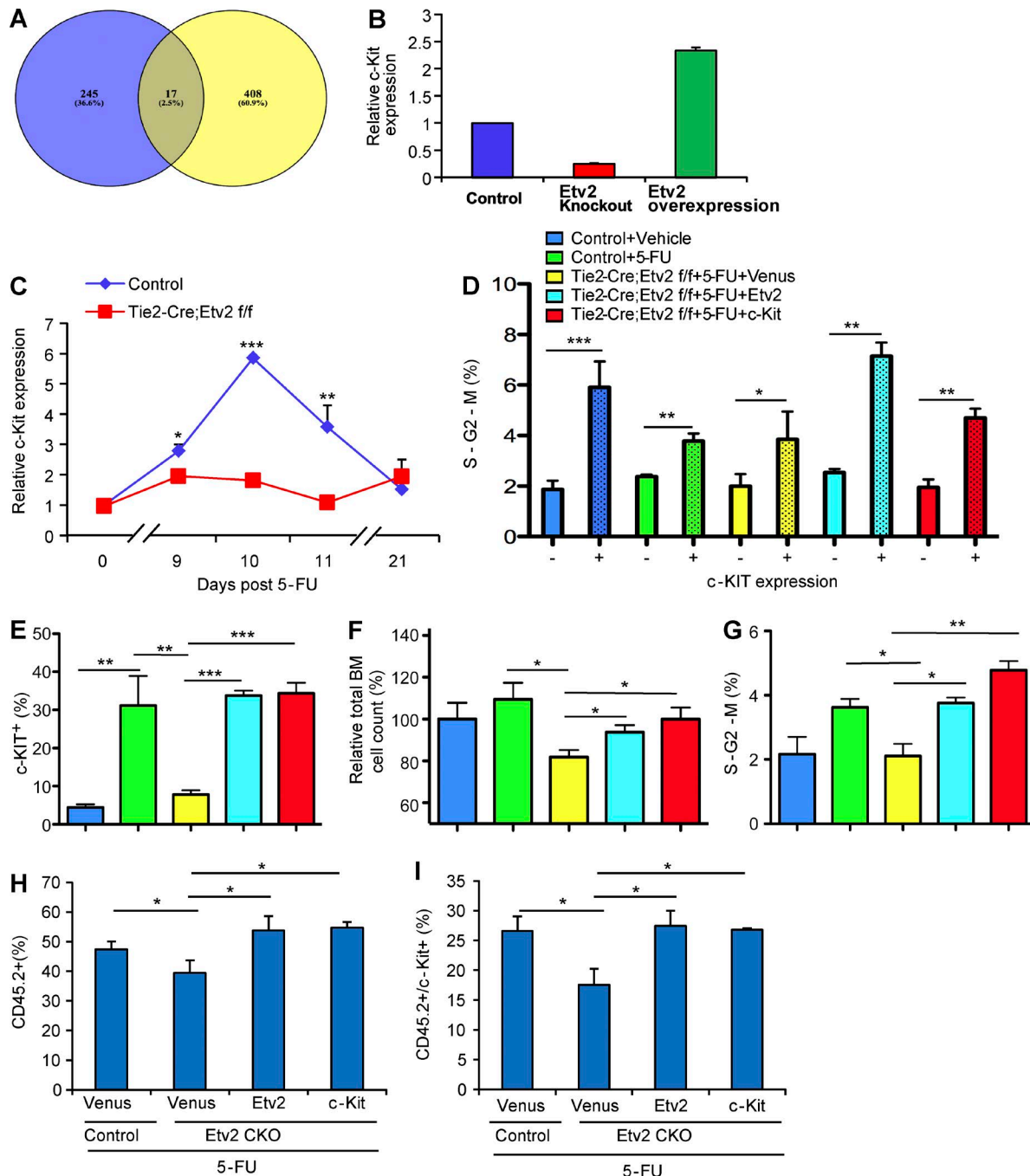


Figure 5. c-Kit is an ETV2 downstream target and responsible for ETV2-mediated HSPC recovery after 5-FU treatment. (A) Among 121 genes that were identified as putative direct targets of ETV2 in differentiated embryonic stem cells by Liu et al. (2015), 17 genes, including *c-Kit*, were annotated as genes related to regulation of cell proliferation. P-value was estimated using hypergeometric distribution. (B) Relative *c-Kit* expression levels, determined by microarray, in control, *Etv2*^{-/-}, or *Etv2*-overexpressing embryoid body (in vitro differentiated embryonic stem) cells is shown (Liu et al., 2012). *n* = 2. (C) Tie2-Cre;*Etv2* CKO or littermate control mice were injected with 250 mg/kg 5-FU i.p. At days 0, 9, 10, 11, and 21, flow cytometry with surface marker staining was performed to determine c-KIT expression levels on Lin⁻ cells after 5-FU injury. Data are expressed as a relative c-KIT expression normalized to the littermate control day-0 group. *n* = 3–5 from two independent experiments. (D–G) Tie2-Cre;*Etv2* CKO or littermate control mice were injected with 250 mg/kg 5-FU. BM mononuclear cells were collected 8 d later and infected with *Venus*, *Etv2*, or *c-Kit* lentivirus for 1 d, followed by cell count and flow cytometry analysis. Cell count was determined by using the CCK8 kit. Five different experimental groups are shown. Blue, control (no 5-FU); green, control + 5-FU; yellow, Tie2-Cre;*Etv2* CKO + 5-FU + lentivirus-*Venus* (*Venus* expressing control lentivirus); cyan, Tie2-Cre;*Etv2* CKO + 5-FU + lentivirus *Etv2*; and red, Tie2-Cre;*Etv2* CKO + 5-FU + lentivirus *c-Kit*. (D) The percentage of c-KIT⁻ and c-KIT⁺ cells in the S-G2-M phase in each group is shown. *n* = 9 from three independent experiments. (E) The frequency of c-KIT-positive cell population in each group is shown. *n* = 9 from three independent experiments.

ies by Shin et al. (2014) and Grinenko et al. (2014), which demonstrated that high c-KIT expression leads to deficits in long-term reconstitution potential. Presumably, lentiviral *c-Kit* expression in *Etv2* KO KSL cells that resulted in high c-KIT expression levels might have caused rescue failure of the long-term repopulation potential. Alternatively, it is also possible that additional ETV2 downstream signaling might be required for rescue of long-term repopulation potential. Future studies on the relationship between ROS and *Etv2* activation as well as *c-Kit* regulation mechanisms are warranted. In conclusion, our research may provide a novel potential target for improving hematopoietic recovery after chemotherapy and hematopoietic transplantation.

MATERIALS AND METHODS

Mice

The generation of *Tie2-Cre;Etv2^{fl/fl}*, *VEC-Cre;Etv2^{fl/fl}*, and *Vav-Cre;Etv2^{fl/fl}* mice has been previously described (Park et al., 2016). In brief, *Tie2-Cre;Etv2^{fl/+}*, *VEC-Cre;Etv2^{fl/+}*, or *Vav-Cre;Etv2^{fl/+}* mice were mated with *Etv2^{fl/fl}* to obtain *Tie2-Cre;Etv2^{fl/fl}*, *VEC-Cre;Etv2^{fl/fl}*, or *Vav-Cre;Etv2^{fl/fl}* mice. *Cre⁺;Etv2^{fl/+}*, *Cre⁻;Etv2^{fl/+}*, or *Cre⁻;Etv2^{fl/fl}* littermates were used as controls. Animal husbandry, generation, and handling were performed in accordance with protocols approved by the Institutional Animal Care and Use Committee of Washington University School of Medical in St. Louis. Information on genotyping primers was previously described (Park et al., 2016).

Competitive BM transplantation

Recipient mice were lethally irradiated (9.5 Gy; single dose) 1 d before cell transplantation. For primary competitive transplantation, 10^6 donor BM cells or 10^4 donor sorted HSPCs (KSL) cells (all are CD45.2) from *Vav-Cre;Etv2* CKO or *VEC-Cre;Etv2* CKO mice were transplanted along with 10^6 BM cells or 10^4 sorted KSL cells as competitor cells from WT mice (CD45.1). The cell suspensions in a 100- μ l volume of PBS were injected into lethally irradiated recipients ($CD45.1 \times CD45.2$) through the retroorbital sinus. In assessing *Etv2* for its endothelial niche requirements, 2×10^6 WT BM cells ($CD45.1 \times CD45.2$) were transplanted into lethally irradiated WT recipients or *VEC-Cre;Etv2* CKO recipients (both are CD45.2). 6 mo after primary transplantation, BM was recovered from the primary recipients, and then, 2×10^6 BM cells ($CD45.1 \times CD45.2$) from primary recipients

were transplanted along with 5×10^5 competitor BM cells (CD45.1) through the retroorbital sinus. PB from recipients was analyzed for donor-derived hematopoiesis by determining the percentage of CD45.1⁺, CD45.2⁺, or CD45.1⁺/CD45.2⁺ PB leukocytes every 4 wk.

5-FU treatment

Control or *Etv2* CKO mice were injected i.p. with a single dose of 5-FU (150 mg/kg or 250 mg/kg; Sigma-Aldrich) or vehicle control (sterile PBS). In serial 5-FU experiments, mice were injected (250 mg/kg each time) for three times at an interval of 11 d. Survival was monitored daily.

Complete blood cell count with differential

PB was obtained by retroorbital collection from WT or *Tie2-Cre;Etv2* CKO mice at days 0, 3, 7, 10, and 14 after one dose of 250-mg/kg 5-FU injection i.p. Whole PB cell counts were analyzed using a hematology system (Hemavet 950FS; Drew Scientific).

Flow cytometry and cell sorting

BM cells were prepared by centrifuging femur and tibia at 12,000 *g* for 1 min. All collected cells were treated with ACK red blood cell lysis buffer (Gibco; Thermo Fisher Scientific) before analyses. mAbs against c-Kit (2B8), Sca1 (D7), CD3e (17A2), B220 (RA3-6B2), Ter119 (TER-119), Gr1 (RB6-8C5), CD16/32 (93), CD34 (RAM34), Flt3 (A2F10), CD150 (c15-12f12.2), CD48 (HM48-1), CD45.1 (A20), CD45.2 (104), and Ki67 (B56) were purchased from BD, BioLegend, or eBioscience. Flow cytometric analysis was performed using an LSRFortessa X-20 or FACSCANTO II flow cytometer (BD).

For cell sorting, BM cells were stained with mAbs against CD3, B220, Gr1, and Ter119 lineage markers, followed by negative selection of lineage-negative cells using a magnetic-activated cell-sorting kit (Miltenyi Biotec). Lin⁻-enriched BM cells were stained with mAbs against lineage markers (CD3, B220, Gr1, and Ter119), c-Kit, and Sca1, and KSL cells were sorted using a FACSaria II flow cytometer (BD).

For cell cycle analysis, BM cells were stained using mAbs against c-Kit, Sca1, CD48, CD150, and lineage markers and fixed/permeabilized using Cytofix/Cytoperm (BD). Then, cells were stained with Ki67 and DAPI and analyzed using an LSR Fortessa X-20 or FACSCANTO II flow cytometer. Ki67⁻DAPI⁻ cells were considered to be in G₀, Ki67⁺DAPI⁻ cells in G₁, and Ki67⁺DAPI⁺ cells in S-G₂-M.

(F) The relative percentage of the cell counts in each group normalized to control (no 5-FU injury) is shown. $n = 9$ from three independent experiments. (G) The percentage of cells in the S-G₂-M phase in each group is shown. $n = 9$ from three independent experiments. (H and I) *Tie2-Cre;Etv2^{fl/fl}* or littermate control mice (CD45.2) were injected with 250 mg/kg 5-FU i.p. 7 d after injection, and 20,000 BM mononuclear cells were isolated and seeded onto a V-shape 96-well plate and infected with either lenti-*Venus*, -*Etv2*, or -*c-Kit*. Littermate control BM mononuclear cells were infected with lenti-*Venus* only. On the second day, cells were transplanted into 9 Gy-irradiated recipient mice (CD45.1) together with 20,000 mock-infected WT BM cells (CD45.1). Donor contribution (CD45.2) and c-Kit-positive cells from BM were analyzed by flow cytometry with surface marker and CD45.1 and CD45.2 3 d after transplantation. $n = 6$ from two independent experiments. *, $P < 0.05$; **, $P < 0.01$; ***, $P < 0.001$. Error bars indicate standard deviations.

KSL cell culture and ROS detection

Sorted KSL cells were cultured in 24-well tissue culture plates (20,000 cells/well) in media containing StemSpan serum-free base medium (STEMCELL Technologies), 10% serum (Hyclone), KitL (1% supernatant), Flt3L (1% supernatant), IL-3 (1% supernatant), and thrombopoietin (10 ng/ml; R&D Systems) in the presence or absence of 200 μ M BSO (Sigma-Aldrich) for 2 d. ROS levels were measured by flow cytometry using 1–5 μ M 2'-7'-dichlorodihydrofluorescein diacetate (DCFDA; Sigma-Aldrich) staining. Median of fluorescence intensity was used to assess the relative ROS content.

Lentiviral production and infection

293FT cells were transfected with CSII-EF-MCS-IRES-VENUS, pHIV-MND-IRES-c-Kit, or CSII-EF-MCS-IRES-Etv2, pCAG-HIVgp, and pCMV-VSV-G-RSV-Rev (4:3:1) by using the calcium phosphate method. *c-Kit* lentiviral vector was obtained from G. Challen (Washington University, St. Louis, MO). 16 h after transfection, the media was changed, and cells were cultured for an additional 48 h. Subsequently, supernatant was harvested and concentrated using a Lenti-X-Concentrator (Takara Bio Inc.). The virus titer was determined by the Lenti-X p24 Rapid Titer kit (Takara Bio Inc.). Virus titer was $\sim 3 \times 10^7$ infectious units per milliliter. 10^5 BM cells were seeded into a 24-well plate and infected with 10^6 virus particles mixed with 8 μ g/ml polybrene (Sigma-Aldrich).

Quantitative RT-PCR

KSL cells sorted from control or 5-FU-treated mice were pooled and used (two to three were pooled as a sample). An RNeasy Micro kit (QIAGEN) was used for RNA extraction according to the manufacturer's instruction. cDNA was prepared by using qScript cDNA SuperMix (Quanta Biosciences) according to the manufacturer's protocol. Quantitative real-time PCR primers for *Etv2*, *Gata2*, *Scl*, *Fli1*, *Runx1*, β -actin, and *Gapdh* used in this study are described in our previous studies (Liu et al., 2015; Park et al., 2016).

Statistical analysis

Student *t* test (Prism5; GraphPad Software) was used for statistical analysis of most in vitro and in vivo experiments. For survival analysis, log-rank test or Gehan-Breslow-Wilson test was used for statistical analysis. A *p*-value <0.05 was considered to be significant.

Online supplemental material

Fig. S1 shows representative FACS analysis for HSPC subsets. Fig. S2 shows two potential ETV2 binding sites and the corresponding sequence within the *c-Kit* locus. Fig. S3 shows representative FACS analysis of *c-Kit* expression.

ACKNOWLEDGMENTS

We thank the Choi laboratory members for constructive criticism and discussion. We thank Dr. Grant Challen for the *c-Kit* lentiviral vector.

This work was supported by the American Cancer Society (grant RSG-14-049-01-DMC) and the National Institutes of Health (grants R01HG007354, R01HG007175, R01ES024992, U01CA200060, and U24ES026699 to D. Li and T. Wang; T32 training grant 5 T32 CA 9547-29 to C.-X. Xu; and grants R01HL63736 and R01HL55337 K. Choi).

The authors declare no competing financial interests.

Author contributions: C.-X. Xu and K. Choi conceived and designed experiments, analyzed data, and wrote the paper. C.-X. Xu with the help of T.J. Lee, N. Sakurai, K. Krchma, and F. Liu performed experiments and analyzed data. D. Li and T. Wang helped with microarray and ChIP-Seq data analysis.

Submitted: 17 June 2016

Revised: 13 February 2017

Accepted: 20 March 2017

REFERENCES

- Busch, K., K. Klapproth, M. Barile, M. Flossdorf, T. Holland-Letz, S.M. Schlenner, M. Reth, T. Höfer, and H.R. Rodewald. 2015. Fundamental properties of unperturbed haematopoiesis from stem cells in vivo. *Nature*. 518:542–546. <http://dx.doi.org/10.1038/nature14242>
- De Val, S., and B.L. Black. 2009. Transcriptional control of endothelial cell development. *Dev. Cell*. 16:180–195. <http://dx.doi.org/10.1016/j.devcel.2009.01.014>
- Ding, L., T.L. Saunders, G. Enikolopov, and S.J. Morrison. 2012. Endothelial and perivascular cells maintain haematopoietic stem cells. *Nature*. 481:457–462. <http://dx.doi.org/10.1038/nature10783>
- Essers, M.A., S. Offner, W.E. Blanco-Bose, Z. Waibler, U. Kalinke, M.A. Duchosal, and A. Trumpp. 2009. IFN α activates dormant haematopoietic stem cells in vivo. *Nature*. 458:904–908. <http://dx.doi.org/10.1038/nature07815>
- Ferdous, A., A. Caprioli, M. Iacovino, C.M. Martin, J. Morris, J.A. Richardson, S. Latif, R.E. Hammer, R.P. Harvey, E.N. Olson, et al. 2009. Nkx2-5 transactivates the *Ets-related protein 71* gene and specifies an endothelial/endocardial fate in the developing embryo. *Proc. Natl. Acad. Sci. USA*. 106:814–819. <http://dx.doi.org/10.1073/pnas.0807583106>
- Gauron, C., C. Rampon, M. Bouzaffour, E. Ipendey, J. Teillon, M. Volovitch, and S. Vrız. 2013. Sustained production of ROS triggers compensatory proliferation and is required for regeneration to proceed. *Sci. Rep.* 3:2084. <http://dx.doi.org/10.1038/srep02084>
- Geissler, E.N., M.A. Ryan, and D.E. Housman. 1988. The dominant-white spotting (*W*) locus of the mouse encodes the *c-kit* proto-oncogene. *Cell*. 55:185–192. [http://dx.doi.org/10.1016/0092-8674\(88\)90020-7](http://dx.doi.org/10.1016/0092-8674(88)90020-7)
- Grinenko, T., K. Arndt, M. Portz, N. Mende, M. Günther, K.N. Cosgun, D. Alexopoulou, N. Lakshmanaperumal, I. Henry, A. Dahl, and C. Waskow. 2014. Clonal expansion capacity defines two consecutive developmental stages of long-term hematopoietic stem cells. *J. Exp. Med.* 211:209–215. <http://dx.doi.org/10.1084/jem.20131115>
- Hameed, L.S., D.A. Berg, L. Belnoue, L.D. Jensen, Y. Cao, and A. Simon. 2015. Environmental changes in oxygen tension reveal ROS-dependent neurogenesis and regeneration in the adult newt brain. *eLife*. 4:e08422. <http://dx.doi.org/10.7554/eLife.08422>
- Huang, E., K. Nocka, D.R. Beier, T.Y. Chu, J. Buck, H.W. Lahm, D. Wellner, P. Leder, and P. Besmer. 1990. The hematopoietic growth factor KL is encoded by the *Sl* locus and is the ligand of the *c-kit* receptor, the gene product of the *W* locus. *Cell*. 63:225–233. [http://dx.doi.org/10.1016/0092-8674\(90\)90303-V](http://dx.doi.org/10.1016/0092-8674(90)90303-V)
- Itkin, T., S. Gur-Cohen, J.A. Spencer, A. Schajnovitz, S.K. Ramasamy, A.P. Kusumbe, G. Lederger, Y. Jung, I. Milo, M.G. Poulos, et al. 2016. Distinct bone marrow blood vessels differentially regulate haematopoiesis. *Nature*. 532:323–328. <http://dx.doi.org/10.1038/nature17624>

- Ito, K., A. Hirao, F. Arai, K. Takubo, S. Matsuoka, K. Miyamoto, M. Ohmura, K. Naka, K. Hosokawa, Y. Ikeda, and T. Suda. 2006. Reactive oxygen species act through p38 MAPK to limit the lifespan of hematopoietic stem cells. *Nat. Med.* 12:446–451. <http://dx.doi.org/10.1038/nm1388>
- Karigane, D., H. Kobayashi, T. Morikawa, Y. Ootomo, M. Sakai, G. Nagamatsu, Y. Kubota, N. Goda, M. Matsumoto, E.K. Nishimura, et al. 2016. p38 α activates purine metabolism to initiate hematopoietic stem/progenitor cell cycling in response to stress. *Cell Stem Cell.* 19:192–204. <http://dx.doi.org/10.1016/j.stem.2016.05.013>
- Kataoka, H., M. Hayashi, R. Nakagawa, Y. Tanaka, N. Izumi, S. Nishikawa, M.L. Jakt, H. Tarui, and S. Nishikawa. 2011. ETV2/ER71 induces vascular mesoderm from Flk1⁺PDGFR α ⁺ primitive mesoderm. *Blood.* 118:6975–6986. <http://dx.doi.org/10.1182/blood-2011-05-352658>
- Kimura, Y., B. Ding, N. Imai, D.J. Nolan, J.M. Butler, and S. Rafii. 2011. c-Kit-mediated functional positioning of stem cells to their niches is essential for maintenance and regeneration of adult hematopoiesis. *PLoS One.* 6:e26918. <http://dx.doi.org/10.1371/journal.pone.0026918>
- Lee, D., C. Park, H. Lee, J.J. Lugas, S.H. Kim, E. Arentson, Y.S. Chung, G. Gomez, M. Kyba, S. Lin, et al. 2008. ER71 acts downstream of BMP, Notch, and Wnt signaling in blood and vessel progenitor specification. *Cell Stem Cell.* 2:497–507. <http://dx.doi.org/10.1016/j.stem.2008.03.008>
- Lee, D., T. Kim, and D.S. Lim. 2011. The Er71 is an important regulator of hematopoietic stem cells in adult mice. *Stem Cells.* 29:539–548. <http://dx.doi.org/10.1002/stem.597>
- Liu, F., I. Kang, C. Park, L.W. Chang, W. Wang, D. Lee, D.S. Lim, D. Vittet, J.M. Nerbonne, and K. Choi. 2012. ER71 specifies Flk-1⁺ hemangiogenic mesoderm by inhibiting cardiac mesoderm and Wnt signaling. *Blood.* 119:3295–3305. <http://dx.doi.org/10.1182/blood-2012-01-403766>
- Liu, F., D. Li, Y.Y. Yu, I. Kang, M.J. Cha, J.Y. Kim, C. Park, D.K. Watson, T. Wang, and K. Choi. 2015. Induction of hematopoietic and endothelial cell program orchestrated by ETS transcription factor ER71/ETV2. *EMBO Rep.* 16:654–669. <http://dx.doi.org/10.15252/embr.201439939>
- Love, N.R., Y. Chen, S. Ishibashi, P. Kritsiligkou, R. Lea, Y. Koh, J.L. Gallop, K. Dorey, and E. Amaya. 2013. Amputation-induced reactive oxygen species are required for successful *Xenopus* tadpole tail regeneration. *Nat. Cell Biol.* 15:222–228. <http://dx.doi.org/10.1038/ncb2659>
- Ludin, A., S. Gur-Cohen, K. Golan, K.B. Kaufmann, T. Itkin, C. Medaglia, X.J. Lu, G. Ledergor, O. Kollet, and T. Lapidot. 2014. Reactive oxygen species regulate hematopoietic stem cell self-renewal, migration and development, as well as their bone marrow microenvironment. *Antioxid. Redox Signal.* 21:1605–1619. <http://dx.doi.org/10.1089/ars.2014.5941>
- Matsui, Y., K.M. Zsebo, and B.L. Hogan. 1990. Embryonic expression of a haematopoietic growth factor encoded by the *Sl* locus and the ligand for c-kit. *Nature.* 347:667–669. <http://dx.doi.org/10.1038/347667a0>
- McLean, C.Y., D. Bristol, M. Hiller, S.L. Clarke, B.T. Schaar, C.B. Lowe, A.M. Wenger, and G. Bejerano. 2010. GREAT improves functional interpretation of cis-regulatory regions. *Nat. Biotechnol.* 28:495–501. <http://dx.doi.org/10.1038/nbt.1630>
- Morimoto, H., K. Iwata, N. Ogonuki, K. Inoue, O. Atsuo, M. Kanatsu-Shinohara, T. Morimoto, C. Yabe-Nishimura, and T. Shinohara. 2013. ROS are required for mouse spermatogonial stem cell self-renewal. *Cell Stem Cell.* 12:774–786. <http://dx.doi.org/10.1016/j.stem.2013.04.001>
- Neuhaus, H., F. Müller, and T. Hollemann. 2010. *Xenopus er71* is involved in vascular development. *Dev. Dyn.* 239:3436–3445. <http://dx.doi.org/10.1002/dvdy.22487>
- Park, C., T.J. Lee, S.H. Bhang, F. Liu, R. Nakamura, S.S. Oladipupo, I. Pitha-Rowe, B. Capoccia, H.S. Choi, T.M. Kim, et al. 2016. Injury-mediated vascular regeneration requires endothelial ER71/ETV2. *Arterioscler. Thromb. Vasc. Biol.* 36:86–96. <http://dx.doi.org/10.1161/ATVBAHA.115.306430>
- Pirotte, N., A.S. Stevens, S. Fraguas, M. Plusquin, A. Van Roten, F. Van Belleghem, R. Paesen, M. Ameloot, F. Cebrià, T. Artois, and K. Smeets. 2015. Reactive oxygen species in planarian regeneration: An upstream necessity for correct patterning and brain formation. *Oxid. Med. Cell. Longev.* 2015:392476. <http://dx.doi.org/10.1155/2015/392476>
- Rasmussen, T.L., J. Kweon, M.A. Diekmann, F. Belema-Bedada, Q. Song, K. Bowlin, X. Shi, A. Ferdous, T. Li, M. Kyba, et al. 2011. ER71 directs mesodermal fate decisions during embryogenesis. *Development.* 138:4801–4812. <http://dx.doi.org/10.1242/dev.070912>
- Salanga, M.C., S.M. Meadows, C.T. Myers, and P.A. Krieg. 2010. ETS family protein ETV2 is required for initiation of the endothelial lineage but not the hematopoietic lineage in the *Xenopus* embryo. *Dev. Dyn.* 239:1178–1187. <http://dx.doi.org/10.1002/dvdy.22277>
- Sato, T., N. Onai, H. Yoshihara, F. Arai, T. Suda, and T. Ohteki. 2009. Interferon regulatory factor-2 protects quiescent hematopoietic stem cells from type I interferon-dependent exhaustion. *Nat. Med.* 15:696–700. <http://dx.doi.org/10.1038/nm.1973>
- Säwén, P., S. Lang, P. Mandal, D.J. Rossi, S. Soneji, and D. Bryder. 2016. Mitotic history reveals distinct stem cell populations and their contributions to hematopoiesis. *Cell Reports.* 14:2809–2818. <http://dx.doi.org/10.1016/j.celrep.2016.02.073>
- Shin, J.Y., W. Hu, M. Naramura, and C.Y. Park. 2014. High c-Kit expression identifies hematopoietic stem cells with impaired self-renewal and megakaryocytic bias. *J. Exp. Med.* 211:217–231. <http://dx.doi.org/10.1084/jem.20131128>
- Sumanas, S., and K. Choi. 2016. ETS transcription factor ETV2/ER71/Etsrp in hematopoietic and vascular development. *Curr. Top. Dev. Biol.* 118:77–111. <http://dx.doi.org/10.1016/bs.ctdb.2016.01.005>
- Sumanas, S., and S. Lin. 2006. Ets1-related protein is a key regulator of vasculogenesis in zebrafish. *PLoS Biol.* 4:e10. <http://dx.doi.org/10.1371/journal.pbio.0040010>
- Sumanas, S., G. Gomez, Y. Zhao, C. Park, K. Choi, and S. Lin. 2008. Interplay among Etsrp/ER71, Scl, and Alk8 signaling controls endothelial and myeloid cell formation. *Blood.* 111:4500–4510. <http://dx.doi.org/10.1182/blood-2007-09-110569>
- Sun, J., A. Ramos, B. Chapman, J.B. Johnnidis, L. Le, Y.J. Ho, A. Klein, O. Hofmann, and F.D. Camargo. 2014. Clonal dynamics of native haematopoiesis. *Nature.* 514:322–327. <http://dx.doi.org/10.1038/nature13824>
- Thorén, L.A., K. Liuba, D. Bryder, J.M. Nygren, C.T. Jensen, H. Qian, J. Antonchuk, and S.E. Jacobsen. 2008. Kit regulates maintenance of quiescent hematopoietic stem cells. *J. Immunol.* 180:2045–2053. <http://dx.doi.org/10.4049/jimmunol.180.4.2045>
- Walter, D., A. Lier, A. Geiselhart, F.B. Thalheimer, S. Huntscha, M.C. Sobotta, B. Moehrl, D. Brocks, I. Bayindir, P. Kaschutnig, et al. 2015. Exit from dormancy provokes DNA-damage-induced attrition in haematopoietic stem cells. *Nature.* 520:549–552. <http://dx.doi.org/10.1038/nature14131>
- Wareing, S., A. Mazan, S. Pearson, B. Göttgens, G. Lacaud, and V. Kouskoff. 2012. The Flk1-Cre-mediated deletion of ETV2 defines its narrow temporal requirement during embryonic hematopoietic development. *Stem Cells.* 30:1521–1531. <http://dx.doi.org/10.1002/stem.1115>

SUPPLEMENTAL MATERIAL

Xu et al., <https://doi.org/10.1084/jem.20160923>

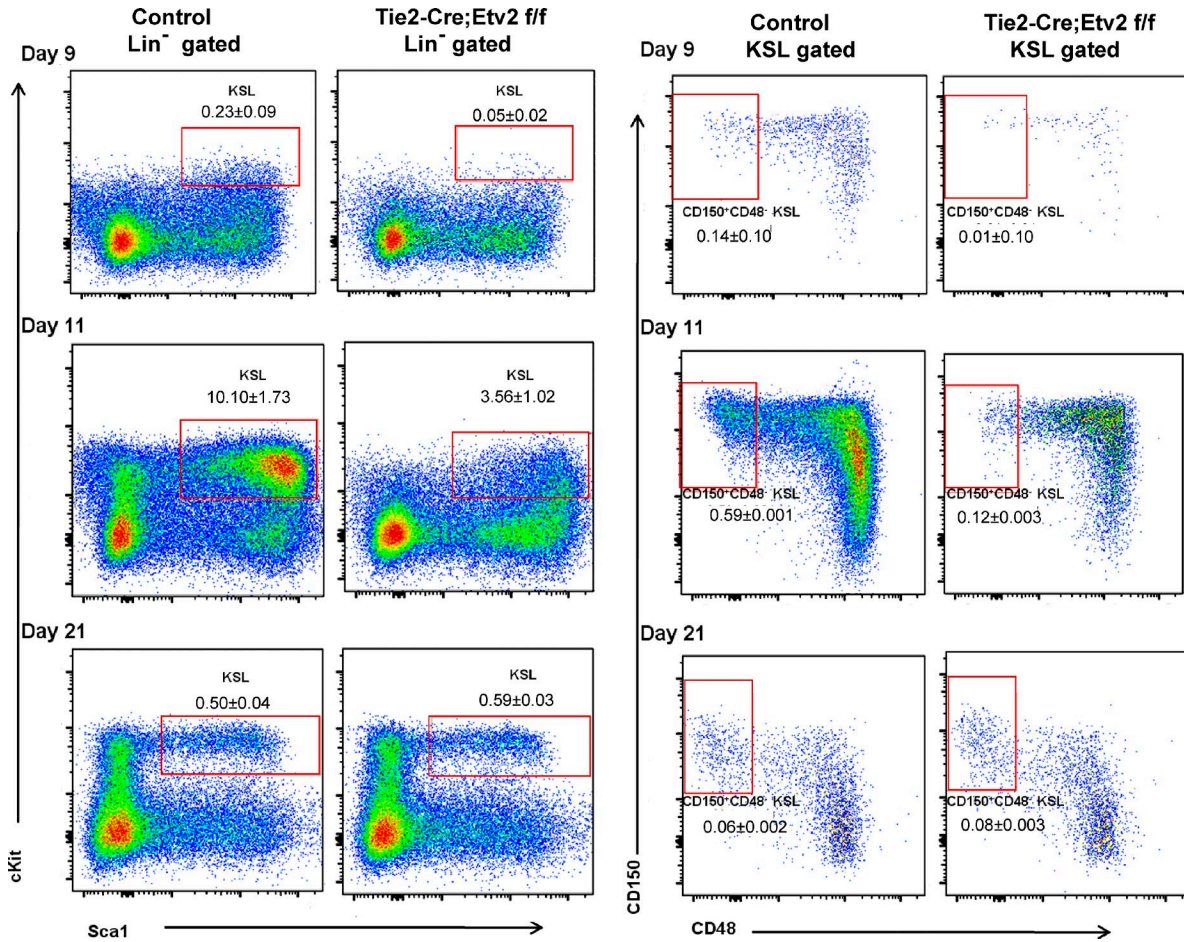


Figure S1. *Etv2* CKO mice display defects in hematopoietic recovery after 5-FU injury (related to Fig. 2). Representative FACS plots of the KSL (c-Kit⁺Sca1⁺Lin⁻) and KSL-SLAM (CD48⁻CD150⁺ KSL) analysis in Tie2-Cre;*Etv2* CKO or control mice after 5-FU treatment are shown. Numbers in the boxes indicate the frequency of KSL cells (left) and CD150⁺CD48⁻ KSL cells (right).

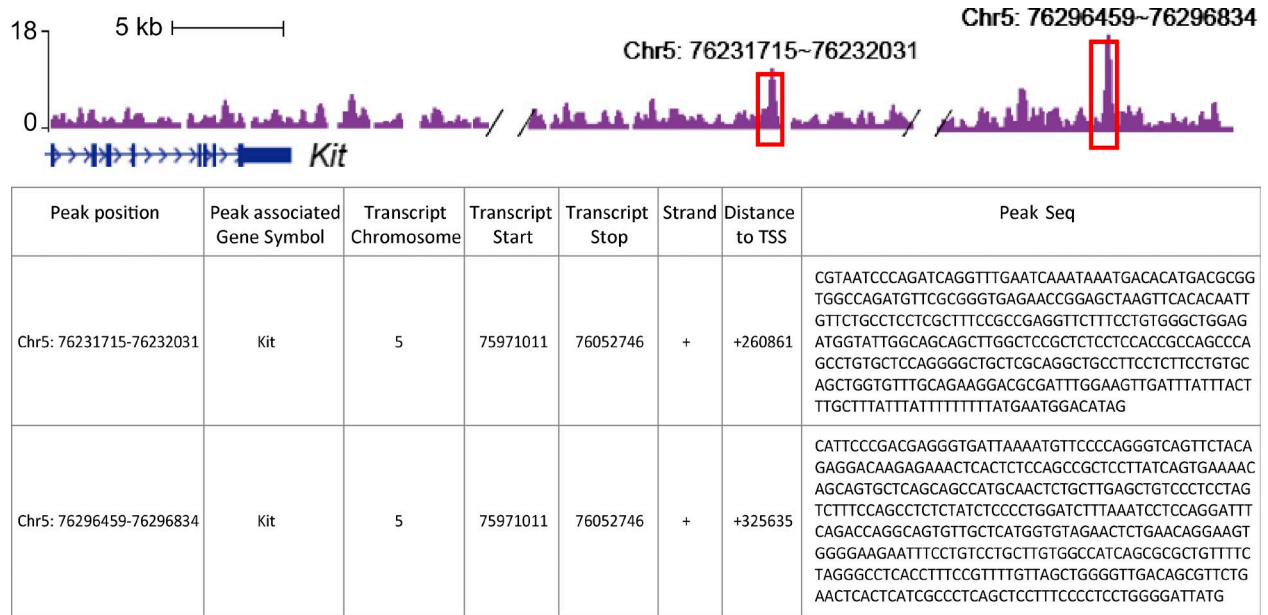


Figure S2. The potential binding sites of ETV2 in the *c-Kit* locus are shown (related to Fig. 5). Two potential ETV2-binding peaks and the corresponding sequences, identified from the ChIP-Seq analysis, are shown (Liu et al., 2015). TSS, transcription start site.

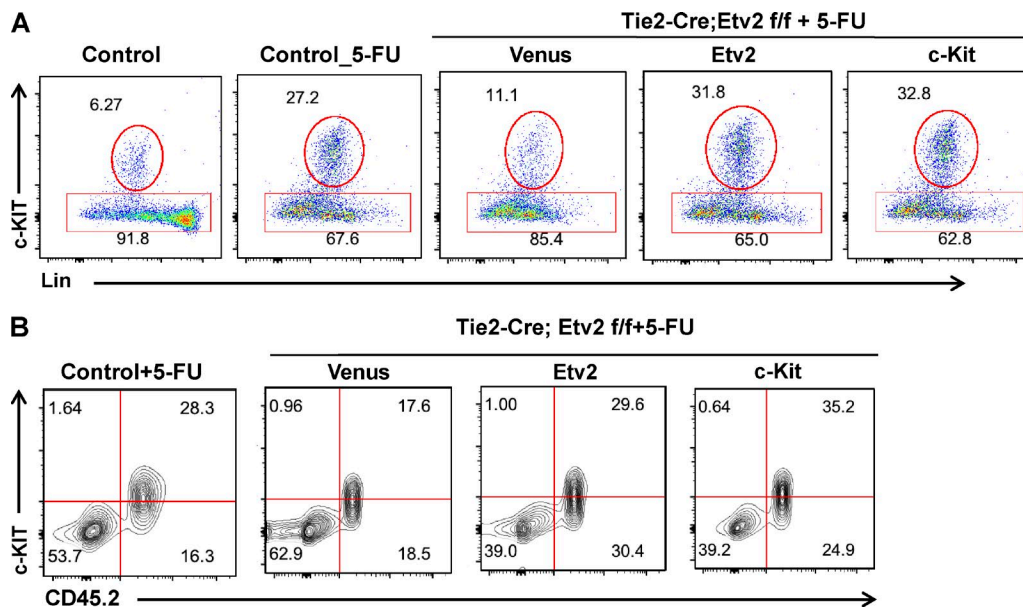


Figure S3. *c-Kit* is downstream of ETV2 in hematopoietic regeneration (related to Fig. 5). (A) Representative FACS plots showing the percentage of *c-KIT*⁺*Lin*^{low/-} cells recovered from the culture after infection with lenti-Venus, -Etv2, or -*c-Kit* virus. (B) Representative FACS plots showing the percentage of donor contribution and CD45.2 and *c-KIT*⁺ cells is shown. BM from Tie2-Cre;Etv2^{ff} mice were obtained 7 d after 5-FU injection, infected with lenti-Venus, -Etv2, or -*c-Kit*, and then competitively transplanted with mock-infected WT BM into 9 Gy-irradiated recipient mice (CD45.1). Littermate control BM was used as the positive control. BM was analyzed 3 d later.